J. Adhesion Sci. Technol., Vol. 21, No. 11, pp. 1097–1116 (2007)

Also available online - www.brill.nl/jast

Characterizing the mechanism of improved adhesion of modified wood plastic composite (WPC) surfaces

GLORIA S. OPORTO [1,2,*], DOUGLAS J. GARDNER [1], GEORGE BERNHARDT [3] and DAVID J. NEIVANDT [4]

[1] *Advanced Engineered Wood Composite (AEWC) Center, University of Maine, Orono, ME 04469, USA*
[2] *Centro de Investigación de Polímeros Avanzados-CIPA, Universidad de Concepción, Edmundo Larenas 234, Concepción, Chile*
[3] *Laboratory for Surface Science and Technology, University of Maine, Orono, ME 04469, USA*
[4] *Department of Chemical and Biological Engineering, University of Maine, Orono, ME 04469, USA*

Received in final form 29 June 2007

Abstract—To have a better knowledge of the phenomena that affect the adhesion characteristics of wood plastic composites (WPCs) a series of surface treatments was performed. The treatments consisted of chemical, mechanical, energetic, physical, and a combination of energetic and physical WPC surface modifications. After each treatment, the composite boards were bonded using a commercial epoxy adhesive, and bond shear strength was determined according to ASTM D 905. All the surface treatments, except the mechanical one, were performed and presented in a previous paper (W. Gramlich *et al*., *J. Adhesion Sci. Technol.* **20**, 1873–1887 (2006)). Mechanical treatment and surface characterization for all the treatments were performed in the present study. The surface characterization included application of thermodynamic and spectroscopic techniques. Most of the surface treatments improved the adhesive bondability of wood plastic composites and, particularly, the smoothest WPC surfaces increased the shear strength by 100% with respect to the control. Thermodynamic measurements indicate that the WPCs low surface energy of about 25 mJ/m^2, is likely due principally to the surface migration of a lubricant component used in the extrusion formulation. The surface energy increased over 45% with respect to the control samples after the chemical treatments. X-ray photoelectron spectroscopy analysis indicated that high oxidation levels of the WPC surfaces resulted in high surface energy and high bond shear strength.

Keywords: Adhesion; contact angle; polypropylene; surface modification; surface energy; roughness; wood plastic composites.

*To whom correspondence should be addressed. Tel.: (1-207) 581-2117. Fax: (1-207) 581-2074; e-mail: gloria.oporto@umit.maine.edu

1. INTRODUCTION

Extruded wood plastic composites (WPCs), used in construction, have made major advances in performance, processing and acceptance. Exterior non-structural or semi-structural building products, such as siding, roofing, decking, fencing and window framing, are being introduced in the marketplace at a high rate [1]. The fabrication of laminate beams based on extruded WPCs for structural applications is one of the latest challenges which requires a very good bondability of WPCs. The surface energy of the principal components of WPCs is approximately 29–30 mJ/m^2 for polypropylene resin [2] and 50 mJ/m^2 for wood [3]. For efficient bonding with an epoxy resin, the surface energy should be over 35 mJ/m^2, which corresponds to the surface energy of uncured epoxy resin [2]. If the properties of WPC surfaces are close to wood, then the bondability can be explained through the mechanical interlocking adhesion theory and, in that case, we should modify the porosity or roughness of the surface for improving its bondability. On the other hand, if properties are closer to the thermoplastic or polyolefin resin, modification of the surface through oxidation processes should be a way to improve its surface energy and finally its bondability.

Wet polymer surface treatments based on chromic acid, methanesulfonic acid and nitric acid solutions will oxidize the surface [4, 5]. Other polyolefin surface treatments include organic peroxides and energetic treatments such as γ-radiation, ultraviolet, corona, low-pressure plasma and flame treatments [6–8]. In the flame process, the oxidation proceeds by a free radical mechanism, accompanied by chain scissions and some cross-linking [9–11]. The functionalities introduced by oxidation are hydroxyl, carbonyl and carboxyl groups [6, 12, 13], with a typical oxidation depth of approximately 4–9 nm [13, 14]. Surfaces of WPCs have demonstrated improved bondability after a flame process [8, 15, 16], oxygen plasma [16] and chromic acid treatment [15, 16]. This could be an indication that the surface of WPCs is likely predominantly covered by the polyolefin matrix.

Previous surface characterization of WPCs has included chemical analysis using ATR–FT-IR and wettability using dynamic contact angles with water [16]. For the ATR–FT-IR, the penetration depth of the evanescent wave depends on the indices of refraction of the crystal and sample, the angle of incidence, and also the wavelength of the photon; normally it is on the order of 0.5–3 μm [17]. At this deep level no significant difference in carbonyl concentrations of flame and chromic acid treatments with respect to control samples was found [16]. Conversely, X-ray photoelectron spectroscopy (XPS) has been found useful to determine the concentration of carbon and oxygen atoms and the oxidation state of the topmost nanometer of many surfaces [18, 19]; however, XPS has yet to be extensively employed for investigation of WPC surfaces.

Surface characterization using thermodynamic techniques has been performed by several researchers to determine the contributions of Lifshitz–van der Waals/acid–base interactions and how they contribute to the bondablity of materials to specific adhesives. The van Oss–Chaudhury–Good (vOCG) approach and the Chang model

apply non-polar and polar liquid probes with known electron acceptor (acid) and electron donor (base) parameters to determine solid surface energy components using contact angle measurements [20–23]. Acid–base characterization has been performed for lignocellulosic surfaces [24–27] and for thermoplastic materials [28]. Page *et al.* characterized the surface energies of both the liquid and solid states of two commercial epoxy resins [2]. They found that the Lifshitz–van der Waals components of the surface energy were similar for both epoxy systems, while the acid–base components were found to be slightly different.

The overall goal of the present work was to characterize the mechanism of improved adhesion of modified wood plastic composite (WPC) surfaces. Specifically, the surface characteristics of WPCs after chemical, mechanical, energetic, physical, and a combination of energetic and physical treatments were determined. Chemical treatment consisted of a wet treatment using chromic acid; mechanical modification considered abrasion methods for producing smooth surfaces; energetic treatments were performed using flame treatment and the application of heat to the WPC surfaces; physical modifications included treatment with water, and the combination of physical and energetic treatments considered water–flame (treatment first with water and then with flame) and flame–water (first flame and then water) treatments. Surface characterization of the individual components of the WPCs was carried out to determine which of them contributed most to the total surface energy of the composites. Surface characterization included application of thermodynamic and spectroscopic techniques. Thermodynamic analysis included the vOCG approach and the Chang model for the surface energy analysis through the sessile drop contact angle measurements; three liquids (water, diiodomethane and ethylene glycol) were used in these determinations and the advancing and receding angles were determined. XPS was used to determine chemical changes and the oxidation level of the surface layer of the treated samples.

2. EXPERIMENTAL

WPC boards for surface treatments were prepared using 50.4 wt% pine wood flour (American Wood Fibers (Schofield, WI, USA)), 39.5 wt% polypropylene (BP Amoco, Houston, TX, USA), 2.3 wt% Polybond 3200 coupling agent (Chemtura, Middlebury, CT, USA), 4.4 wt% TPW 113 lubricant (Struktol, Stow, OH, USA), and 3.4 wt% gray colorant (Clariant, Lewiston, ME, USA). These raw materials were extruded using a Davis-Standard WT94 Twin Screw Extruder to produce WPC boards about 2.5 m to 3 m (long), 14 cm (wide) and 4 cm (thick). The boards were planed on both faces to provide a flat region for adhesion to occur, and then, they were cut to obtain bonding samples of approximately 50 cm long. Finally, the boards were treated chemically, mechanically, energetically, physically, and using a combination of energetic and physical treatments.

2.1. Chemical treatment

WPC boards were treated with chromic acid. A solution of de-ionized water, potassium dichromate and sulfuric acid (98%) was prepared and applied on the board surface. The board surface was completely covered with this solution for a residence time of 5 min. Subsequently, the surfaces were washed with de-ionized water to remove the chemical residues from the treatment. Finally, the wash water was removed with the application of heat from a Model 1220HS Milwaukee heat gun at high power by holding the heat gun 5 cm from the surface of the board and passing it over the board at a rate of approx. 2.5 cm/s [15]. The water and heat treatments used after the chromic acid treatment were evaluated separately to analyze possible synergistic improvements. Water was included as physical treatment and heat was included as energetic treatment.

2.2. Mechanical treatment

WPC boards were sanded using abrasive papers of two different grit sizes, P60 and P220. An Alpha-Step Surface Profilometer with ten nanometer resolution in the z-direction was used for surface roughness determinations. The measurements consisted of three determinations for each sample, performed on a 500 μm line. The resulting roughness averages expressed as the root mean square (R_{rms}) are presented in Table 1. After the surface mechanical treatment, the samples were cleaned with acetone to eliminate any contaminants from the abrasion process.

2.3. Energetic treatment

WPC boards were treated using a flame treatment process and separately by the application of heat on the surface. The flame treatment was performed using a hand-held propane torch with a flame of approximately 7 cm in length, which was passed over the WPC surface. The flame treatment is explained in more detail in the procedure presented by Gardner *et al.* [8] and Gramlich *et al.* [15]. The heat treatment was performed through the application of heat from a heat gun (Model 1220HS Milwaukee) at high power by holding the heat gun 5 cm from the surface of the board and passing it over the board at a rate of approx. 2.5 cm/s.

Table 1.
Root mean square (rms) roughness after mechanical treatments

Sample	R_{rms} (μm)
Control	5.60
P60	2.60
P220	1.43

2.4. Physical treatment

WPC boards were submerged in de-ionized water for 10 min; then they were dried with absorbent paper and the residual water was removed using a heat gun as described above.

2.5. Combination of energetic and physical treatments

WPC boards were modified using a combination of water–flame and flame–water treatments. For water–flame treatment the boards were treated with water, as described in Section 2.4, and then the flame treatment was performed on the surface. Conversely, for flame–water treatment the flame treatment was performed first, as described in Section 2.3, and then the water treatment was applied [15].

2.6. Adhesive application

An epoxy adhesive consisting of Pro-Set® M1013 resin with M2017 Pro-Set® hardener manufactured by Gougeon Brothers (Bay City, MI, USA) was employed. The epoxy adhesive was prepared by mixing 25.7 g resin and 6.3 g hardener and applied to the treated surface of one board. A second treated board was place on top of the adhesive and they were pressed applying a load of 3.52 kg/cm^2. The samples were kept in the press for at least 8 h at that pressure and at room temperature to ensure a complete cure of the adhesive.

2.7. Shear strength measurements

The adhesively bonded boards were cut into shear block samples (specimens) according to ASTM D905. A minimum of 20 specimens per treatment were prepared and then kept for five days in the Material Testing Laboratory at the AEWC Center to equilibrate to the test environment prior to the adhesive shear strength testing at 18°C and 50% relative humidity. The specimens were tested according to ASTM D905 using a Tinius Olsen Testing Machine Model 87551 shear block test fixture. The maximum load for each sample was recorded upon sample failure, and the bondline examined to determine the percentage of the bondline or composite failure. As discussed in an earlier paper [15], material failure was defined as the percentage of composite contacting the adhesive that remained in the bondline after testing; as such material failure is a measure of the affinity of the composite for the epoxy. Conversely, the presence of wood in the bondline after testing was evaluated to determine the affinity of the wood component present in the WPCs for the epoxy resin.

2.8. Contact angle and surface energy determinations of WPCs surfaces

The sessile-drop method was chosen for contact angle measurements and the advancing and receding contact angle were determined. Advancing angle was

Table 2.
Surface free energy parameters (in mJ/m^2) for the probe liquids used for contact angle determinations according to the vOCG aproach

Liquid	γ_L	γ_L^{LW}	γ_L^{AB}	γ_L^+	γ_L^-
Diiodomethane	50.8	50.8	0	0	0
Ethylene glycol	48.0	29.0	19.0	1.9	47.0
Water	72.8	21.8	51.0	25.5	25.5

Table 3.
Surface free energy parameters for the probe liquids used for contact angle determinations according to the Chang model

Liquid	γ_L (mJ/m^2)	γ_L^{LW} (mJ/m^2)	γ_L^{AB} (mJ/m^2)	P_L^A (mJ/m^2)$^{1/2}$	P_L^B (mJ/m^2)$^{1/2}$
Diiodomethane	50.8	50.8	0.0	0.0	0.0
Ethylene glycol	48.0	28.1	20.1	3.69	−5.44
Water	72.8	21.8	50.9	6.88	−7.40

determined after the first 10 s of the droplet on the surface, and the receding angle was determined as the angle formed by the droplet just before the evaporation, where the contact angle is constant and the droplet base radius diminishes [29]. Hysteresis was calculated as the difference between the advancing and receding contact angles. Three probe liquids (diiodomethane, water and ethylene glycol) were placed on the surface of the WPC boards. Drops of 5 µl volume were employed and a total of 12 droplets were analyzed for each liquid. The contact angle determinations were performed through the capture of the droplet images using Labview® software and a camera based contact angle analysis system [30]. The images were analyzed by digital image analysis using Matlab®, and the final contact angles were obtained using the Sherlock® software package (Media Cybernetics, Bethesda, MD, USA). For each WPC treatment, surface energy calculations were performed using contact angle data and application of the van Oss–Chaudhury–Good (vOCG) approach and the Chang model [21, 23]. In Tables 2 and 3 the probe liquid parameters used for the determination of the WPC surface energy are listed.

2.9. Contact angle and surface energy determinations of individual components of WPCs

10 g of each individual component used in the WPCs formulation, i.e., polypropylene, lubricant, coupling agent and colorant, were melted separately in a glass Petri dish. A solid flat surface was obtained for each component after it cooled and this was used for contact-angle determinations. The advancing contact-angle determinations and surface energy calculations were performed as mentioned in Section 2.8 for the WPCs surfaces.

2.10. XPS measurements

XPS measurements were conducted on a Specs Phoibos HSA 3000 Plus spectrometer (with hemispherical energy analyzer) having a channeltron electron multiplier. Aluminum was used as the anode. A voltage of 14.5 kV was used to accelerate X-ray photoelectrons at a current of 20 mA. The dimensions of the samples were 4 mm (wide) × 7 mm (long) × 1 mm (thick). The samples were analyzed at a take-off angle of 90°, which corresponded to a penetration depth of 3.7 nm. Survey or low-resolution spectra were recorded from 0 to 1100 eV and high-resolution spectra of the C_{1s} region from 280 to 300 eV and for the O_1 region from 525 to 545 eV were recorded. The resulting spectra were analyzed using CasaXPS software (RBD Enterprises, Bend, OR, USA). The ratio of elemental oxygen to carbon (O/C) was determined from the low-resolution spectra. To determine the types of oxygen–carbon bonds present, chemical bond analysis of carbon was accomplished by curve fitting the C_{1s} peak from the high-resolution spectra and deconvoluting it into four subpeaks corresponding to unoxidized carbon, C_1 (285.0 eV), and various oxidized carbons, C_2, C_3 and C_4 using CasaXPS software. An oxidized to unoxidized carbon ratio ($C_{oxidized}/C_{unoxidized}$) was calculated using equation (1).

$$C_{oxidized}/C_{unoxidized} = (C_2 + C_3 + C_4)/C_1. \quad (1)$$

3. RESULTS

3.1. Contact angle and surface energy determinations

The advancing and receding contact angles were determined for WPC control surfaces (without treatment) for the three probe liquids (diiodomethane, water and ethylene glycol). It was found that evaporation occurred only for the water probe liquid on the WPC surface. The receding contact angle in this case was determined when the droplet base radius began to diminish while contact angle was constant [29]. For diiodomethane and ethylene glycol probe liquids evaporation was not a factor; therefore, in future discussion these contact angles correspond to the advancing contact angle. In Fig. 1, the water advancing and receding contact angles for all the WPC treatments and also the hysteresis values, which correspond to the difference between the advancing and receding contact angles are presented. Figure 2 presents the contact angle measurements for all the treatments using diiodomethane (advancing contact angle), water (advancing and receding contact angle) and ethylene glycol (advancing contact angle).

Analysis of variance (ANOVA) was performed to determine significant differences among the contact angles for each probe liquid and for each treatment or group of treatments compared with control samples. P-values were calculated using ANOVA single factor. Accordingly P-values < 0.05 imply statistical significance (SS) in the mean of contact angle measurements among treatments for each probe

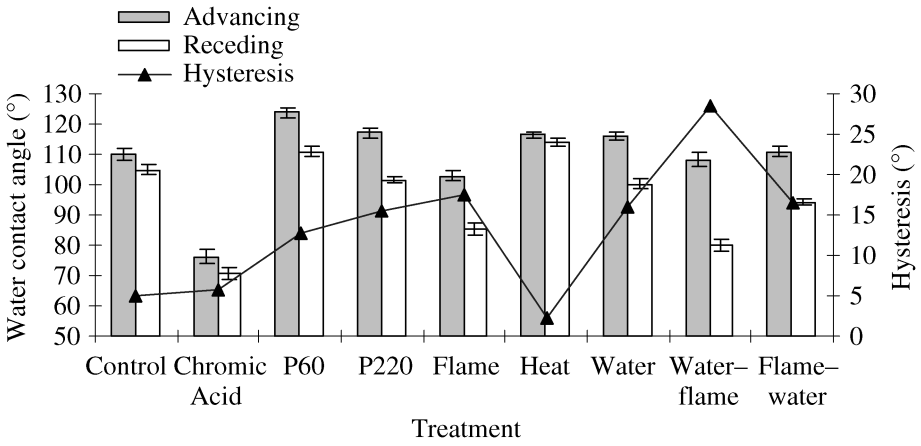

Figure 1. Advancing, receding and contact-angle hysteresis values using water as a probe liquid. Error bar represents the standard error in the mean. The standard error in the mean in the simplest case is defined as the standard deviation divided by the square root of the number of measurements.

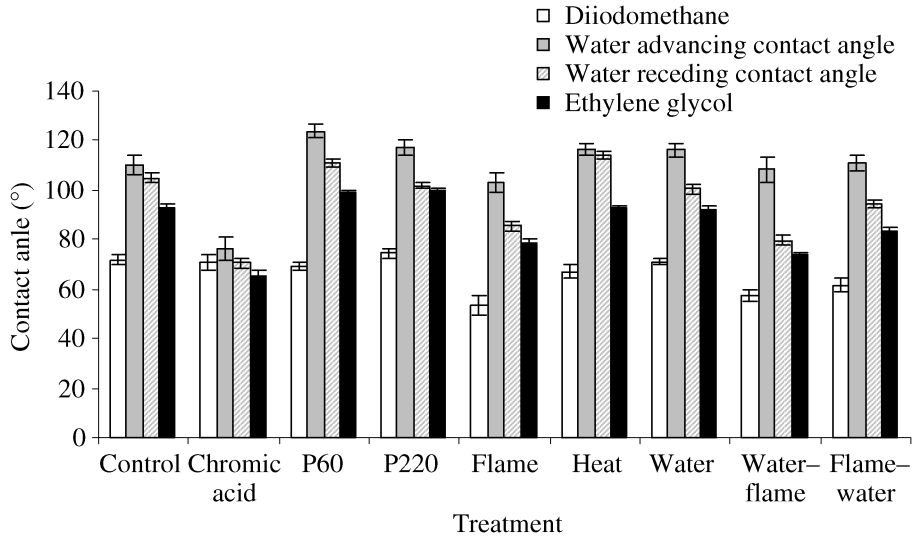

Figure 2. Contact-angle measurements. Error bar represents the standard error in the mean.

liquid; P-values $\geqslant 0.05$ imply no statistical significance (NSS) in the mean of contact angle measurements among treatments for each probe liquid. In Table 4, the indication of statistical significance (SS) or no statistical significance (NSS) among the treatments from their corresponding contact angles are presented. The results indicate that there are statistical significant differences with respect to contact-angle determination (using diiodomethane, water and ethylene glycol) among the control samples and those treated chemically, mechanically, energetically, physically or with a combination of energetic and physical treatments. In some cases, no statisti-

Table 4.
Indication of statistical (SS) or no statistical significance (NSS) according to P-values determination[a] for groups of treatments

	Control and Chemical treatment (Chromic acid)	Control and Mechanical treatments (P60, P220)	Control and Energetic treatments (Flame, Heat)	Control and Physical treatment (Water)	Control and Energetic and physical treatments (Water–flame, Flame–water)
P-value for diiodomethane	NSS	SS	SS	NSS	SS
P-value for water, advancing contact angle	SS	SS	SS	SS	NSS
P-value for water, receding contact angle	SS	NSS	SS	SS	SS
P-value for ethylene glycol	SS	NSS	SS	NSS	SS

[a] P-values were calculated using ANOVA single factor. P-value < 0.05 implies statistical significance (SS) in the mean of contact angle measurements between treatments for each probe liquid. P-value $\geqslant 0.05$ implies no statistical significance (NSS) in the mean of contact angle measurements between treatments for each probe liquid.

cal significant differences were found using individual liquids; however, the surface energy was determined using these three liquids.

The surface energy was calculated for each treatment using the vOCG approach and the Chang model. The resulting values are presented in Tables 5 and 6, respectively, and they were performed using diodomethane (advancing contact angle), water (advancing or receding contact angle) and ethylene glycol (advancing contact angle). The results indicate that for the vOCG approach the highest total surface energy values and the non-polar Lifshitz–van der Waals component of the surface energy (γ_s^{LW}) correspond to flame, flame–water and water–flame treatments. Also, for all the treatments, the acid–base component of the surface energy (γ_s^{AB}) increases when the water receding contact angle is used in the surface energy calculations. For the Chang model, the highest total surface energy corresponds to flame, flame–water and water–flame treatments, as found using the vOCG approach. In addition a high surface energy was found using the Chang model for the chromic acid treatment. For this treatment, the acid–base component of the surface energy is the highest not only when the water receding angle is used, but also when the water advancing angle is used.

In the Chang model, P_S^a and P_S^b correspond to the principal acid–base parameters of the solid; they give an indication of the acidic (if both values are positive), basic (if both values are negative) or amphoteric nature of the surface (if the parameters have opposite signs). According to the results presented in Table 6, the chromic-acid-treated surface presents an amphoteric nature; the rest of the treated surfaces exhibit a basic surface.

An important consideration to keep in mind is the coefficient of correlation (R^2) obtained using the vOCG approach and the Chang model. For the vOCG approach,

Table 5.
Surface energy and its components (in mJ/m^2) according to the vOCG approach

	Control	Chromic acid	P60	P220	Flame	Heat	Water	Water–flame	Flame–water
γ_s^{LW*}	20.8	20.7	22.8	19.4	31.1	23.8	21.9	30.6	27.3
γ_s^{LW**}	20.2	20.0	21.4	18.0	28.7	23.5	20.1	26.8	25.2
γ_s^{AB*}	0.9	4.4	0.7	0.6	0.6	0.0	0.0	0.2	0.0
γ_s^{AB**}	1.9	4.1	2.5	5.5	5.2	0.4	3.3	3.3	3.0
γ_s^{total*}	21.7	25.1	23.5	20.0	31.7	23.8	21.9	30.8	27.3
$\gamma_s^{total**}$	22.1	24.1	23.9	23.5	33.9	23.9	23.4	30.1	28.2
R^{2*}	0.92	0.99	0.99	0.94	0.92	0.97	0.96	0.92	0.97
R^{2**}	0.94	0.99	0.92	0.93	0.96	0.94	0.95	0.97	0.95

* Using diiodomethane (advancing contact angle), water (advancing contact angle) and ethylene glycol (advancing contact angle).

** Using diiodomethane (advancing contact angle), water (receding contact angle) and ethylene glycol (advancing contact angle).

Table 6.
Surface energy parameters according to the Chang model

	Control	Chromic acid	P60	P220	Flame	Heat	Water	Water–flame	Flame–water
γ_s^{LW*} (mJ/m^2)	20.8	20.7	22.8	19.4	31.1	23.8	21.9	30.6	27.3
γ_s^{LW**} (mJ/m^2)	20.2	20.0	21.4	18.0	28.7	23.5	20.1	26.8	25.2
γ_s^{AB*} (mJ/m^2)	−1.0	8.5	−0.6	−1.0	−1.7	−1.3	−1.3	−2.1	−1.7
γ_s^{AB**} (mJ/m^2)	−0.6	11.4	−0.9	0.0	1.0	−1.3	0.0	3.5	0.2
γ_s^{total*} (mJ/m^2)	19.8	29.2	22.2	18.4	29.4	22.5	20.6	28.5	25.6
$\gamma_s^{total**}$ (mJ/m^2)	19.6	31.4	20.5	18.0	29.7	22.2	20.1	30.3	25.4
P_s^{b*} (mJ/m^2)$^{1/2}$	−1.3	−4.1	−0.3	−0.8	−1.6	−0.8	−1.0	−1.6	−1.3
P_s^{b**} (mJ/m^2)$^{1/2}$	−1.6	−4.4	−1.0	−1.6	−2.6	−1.0	−1.9	−3.2	−2.2
P_s^{a*} (mJ/m^2)$^{1/2}$	−0.8	2.1	−2.0	−1.2	−1.1	−1.5	−1.3	−1.3	−1.3
P_s^{a**} (mJ/m^2)$^{1/2}$	−0.4	2.6	−1.0	0.0	0.4	−1.3	0.0	1.1	0.1
R^{2*}	0.83	0.96	0.92	0.32	0.95	0.90	0.99	0.81	0.98
R^{2**}	0.75	0.93	0.51	0.50	0.73	0.77	0.70	0.83	0.78

* Using diiodomethane (advancing contact angle), water (advancing contact angle) and ethylene glycol (advancing contact angle).

** Using diiodomethane (advancing contact angle), water (receding contact angle) and ethylene glycol (advancing contact angle).

all the R^2 values were above 0.90 using both advancing and receding water contact angles. For the Chang model, the R^2 values were over 0.90 only for the chromic acid treatment using both advancing and receding water contact angles. Although the R^2 values were lower for the Chang model, the results were comparable to those of the vOCG approach.

In Figs 3 and 4 the increase in surface energy of the treated samples with respect to the control is presented. The surface energy increased for almost all the treatments when the water advancing or water receding contact angle were used in the determinations. For the vOCG approach there is an increase with statistical

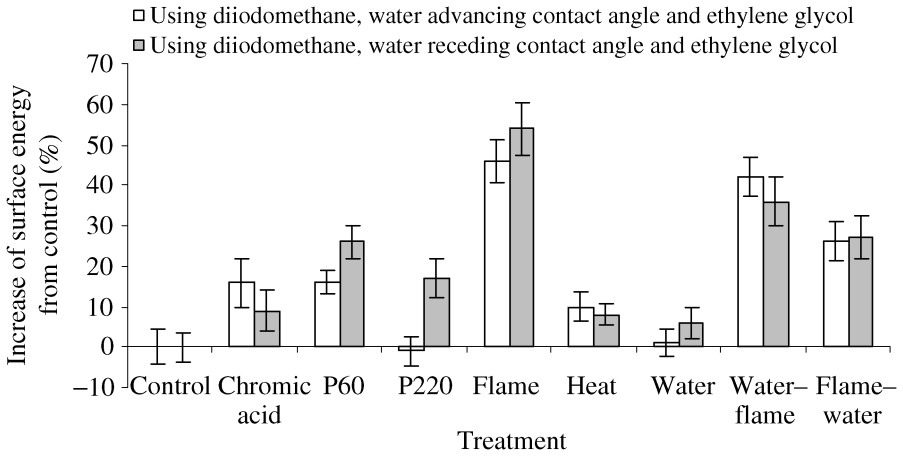

Figure 3. Increase in WPC surface energy compared with the control using the vOCG approach. Error bar represents the propagation of the error (calculated as the sum of the standard errors in the means for the contact-angle determinations).

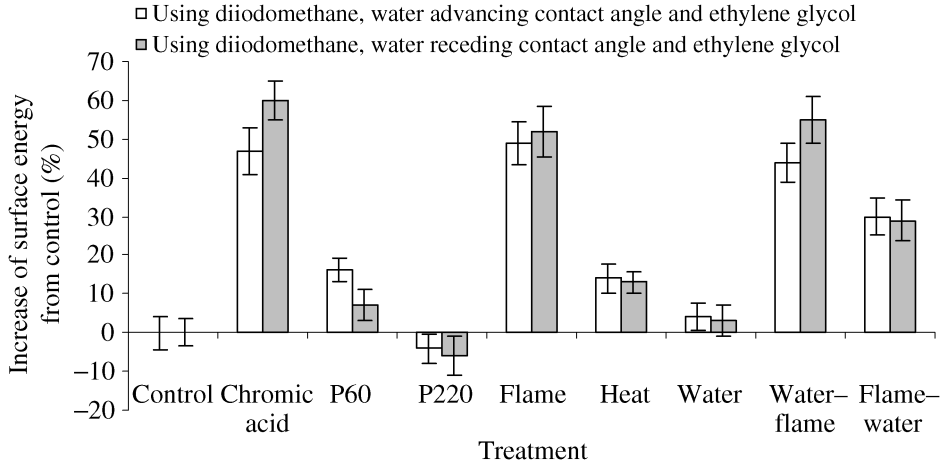

Figure 4. Increase in WPC surface energy compared with the control using the Chang model. Error bar represents the propagation of the error (calculated as the sum of the standard errors in the means for the contact-angle determinations).

significance in the total surface energy for the mechanical treatments (P60 and P200) and for the flame treatments. According to the Chang model, there is an increase with statistical significance in the total surface energy for the chromic acid treatment. Considering the lower coefficients of correlation presented for the Chang model for mechanical treatments (P60, 0.51 and P220, 0.50) no analysis will be presented at this point.

To determine which component(s) of the WPC formulation contributed to the surface energy, which according to the results previously presented is lower than that of polypropylene, determinations of the contact angle and surface energy of the

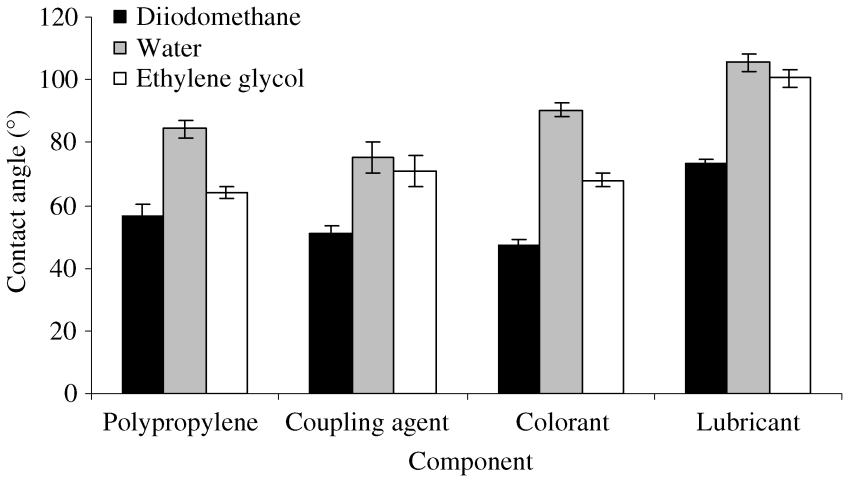

Figure 5. Contact-angle measurements on the WPC components. Error bars represent the standard error in the mean.

Table 7.
Surface energy and its components (in mJ/m^2) for individual components of WPCs according to the vOCG approach

	Polypropylene	Coupling agent	Colorant	Lubricant
γ_s^{LW}	29.0	29.6	34.0	18.7
γ_s^{AB}	1.4	4.9	0.6	4.7
γ_s^{total}	30.4	34.5	34.6	23.4
R^2	0.99	0.97	0.97	0.93

Table 8.
Surface energy and its components for individual components of WPCs according to the Chang model

	Polypropylene	Coupling agent	Colorant	Lubricant
γ_s^{LW} (mJ/m^2)	29.0	29.6	34.0	18.7
γ_s^{AB} (mJ/m^2)	2.3	4.1	−0.6	−0.5
γ_s^{total} (mJ/m^2)	31.2	33.7	33.4	18.2
P_s^b $(mJ/m^2)^{1/2}$	−3.2	−3.4	−2.5	−1.4
P_s^a $(mJ/m^2)^{1/2}$	0.7	1.2	−0.2	−0.3
R^2	0.97	0.80	0.95	0.43

individual components of WPCs were performed. Figure 5 presents the contact angles obtained for polypropylene, coupling agent, colorant and lubricant using the probe liquids diiodomethane, water and ethylene glycol. The resulting surface energies for all of the WPC components are presented in Tables 7 and 8. According to the Chang model, the polypropylene and coupling agent surfaces are amphoteric, while the colorant and lubricant are basic.

The highest contact angle values using the three liquids correspond to the lubricant; these values give the lowest surface energy value of approximately

20.75 mJ/m^2 (average between the vOCG approach and the Chang model), which corresponds closely to the surface energy of the WPCs (20.70 mJ/m^2).

3.2. Shear strength results and material failure results

Table 9 displays the shear strength results after the WPCs surface treatments. All treatments, except for the heat treatment, show an increase in shear strength relative to the control. Figure 6 presents the increase in shear strength compared to control samples for all the treatments. The smoothest surface (P220) displayed a shear strength value higher than flame treated surface and closer to chromic-acid, water–flame- and flame–water-treated surfaces. Table 10 presents the observed average material failure values, which correspond to a measure of the affinity of the composite for the epoxy resin, and the percent of samples with wood present in the bondline, which represents the affinity of the wood component present in the WPCs for the epoxy resin. Results indicate that the control, mechanical (P60 and P220) and heat-treated surfaces show similar values for material failure (0%), but the number of samples with the wood in the bondline is higher for the smoothest

Table 9.
Shear strength results for different WPC surface treatments

WPC surface treatment	Number of samples tested	Shear strength (MPa)	95% confidence interval (MPa)
Control (R_{rms} 5.6 μm)	54	4.49	0.21
Chromic acid	34	8.83	0.23
P60 (R_{rms} 2.6 μm)	50	5.84	0.21
P220 (R_{rms} 1.43 μm)	50	8.98	0.23
Flame	36	7.52	0.26
Heat	36	4.23	0.46
Water	36	5.89	0.28
Water–flame	31	8.12	0.28
Flame–water	34	8.83	0.23

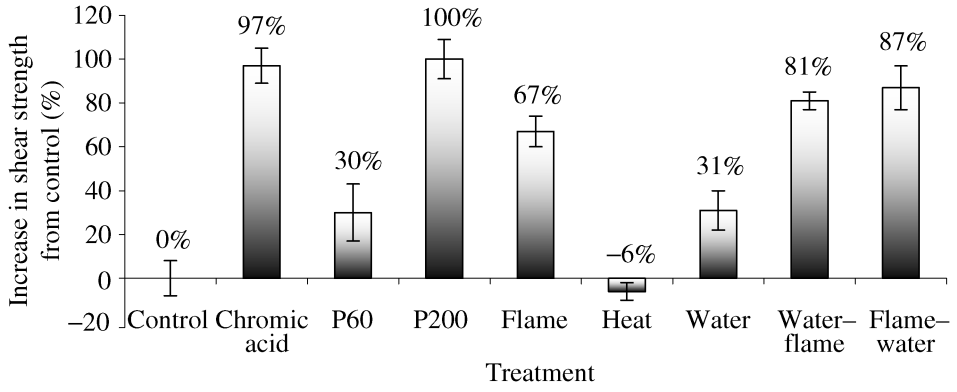

Figure 6. Increase in shear strength from control samples. Error bar represents 95% confidence interval for each treatment.

Table 10.
Observed average material failure and percentage of samples with wood present in the bondline for shear block samples tested

WPC surface treatment	Material failure* (%)	Samples with wood in the bondline** (%)
Control (R_{rms} 5.6 μm)	0	28
Chromic acid	5	0
P60 (R_{rms} 2.6 μm)	0	60
P220 (R_{rms} 1.43 μm)	0	80
Flame	4	94
Heat	0	22
Water	1	78
Water–flame	5	97
Flame–water	7	77

* Measure of the affinity of the composite for the epoxy.
** Measure of the affinity of the wood component present in the WPCs for the epoxy resin.

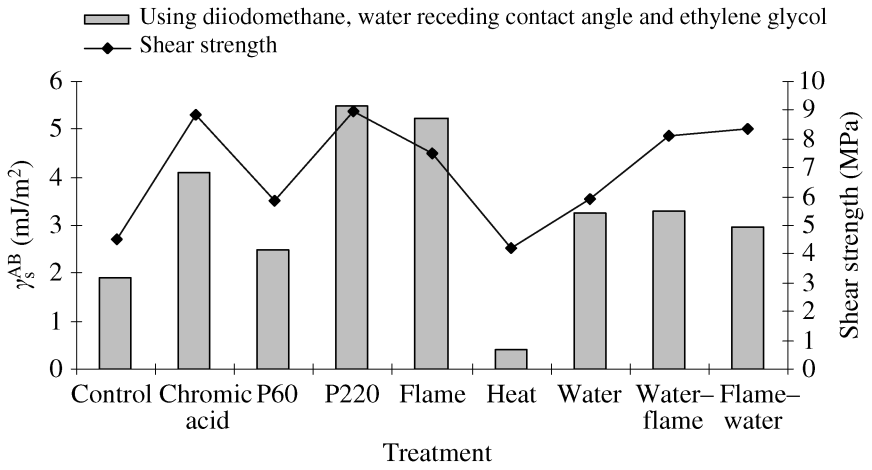

Figure 7. Relationship between the acid–base components of the surface energy (γ_s^{AB}) using the vOCG approach and the shear strength measurements for various WPC surface treatments.

surfaces (P60 (60%) and P220 (80%)) compared to control and heat-treated samples (28% and 22%, respectively). Flame-treated surfaces show similar percentages of samples with wood in the bondline as the water and P220 treatments (78% and 80%, respectively), but also presented higher values for material failure (4%, 5% and 7%) compared to water and P220 treatments (1 and 0%, respectively). Chromic-acid-treated surfaces show a higher material failure (5%), but no samples showed wood in the bondline.

The relationship between the shear strength measurements and the acid–base component of surfaces using the vOCG approach is shown in Figure 7. In general, a lower shear strength corresponded to a lower acid–base component of surface energy.

3.3. XPS

The XPS analyses confirmed the presence of carbon and oxygen on the surface of the WPCs, and allowed quantification of the level of sample oxidation after the treatments at the topmost surface layers. From the deconvolution of the carbon's high resolution spectra it was possible to obtain subpeaks corresponding to unoxidized carbon (C_1=C–H or C–C) and oxidized carbon (C_2, C_3 and C_4, which contained carbon–oxygen bonds as in C–OH, O–C–O, C=O or O–C=O). For the oxygen spectra, only one state was found for all the treated samples. The results are presented in Table 11, and it is evident that the higher the oxygen concentration, the higher the ratio of oxidized carbons to unoxidized carbons. Flame, chromic acid, water–flame and flame–water treatments exhibited increased oxygen on the WPC surface. The relationship between the oxidized carbons to unoxidized carbons, the shear strength, and the surface energy (according to the vOCG approach and the Chang model) is presented in Fig. 8; in Fig. 8 it is noted that the increases in both shear strength and surface energy are associated with a higher level of oxidation on the WPC surfaces.

Table 11.
XPS analysis results

Treatment	Carbon (%)	Oxygen (%)	$C_{unoxidized}$ (%)	$C_{oxidized}$ (%)	$C_{oxidized}/C_{unoxidized}$ (%)
Control	92.0	8.0	92.5	7.5	8.1
Chromic acid	86.9	13.1	76.3	23.7	31.1
Flame	89.6	10.4	87.0	13.6	15.6
Heat	90.5	9.5	95.9	4.1	4.3
Water	92.1	7.9	92.4	7.6	8.2
Water–flame	88.4	11.6	87.8	12.2	13.9
Flame–water	90.5	9.5	86.8	13.2	15.2

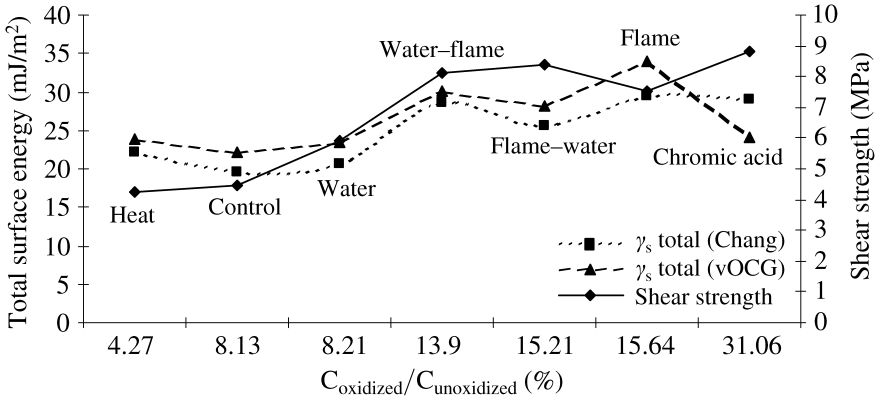

Figure 8. Relationship between total surface energy (according to the vOCG approach and the Chang model), shear strength and the $C_{oxidized}$ to $C_{unoxidized}$ ratio.

4. DISCUSSION

The diiodomethane contact angles of WPCs reflect the non-polar Lifshitz–van der Waals component in the vOCG surface energy approach. Particularly for the flame, water–flame and flame–water treatments, which exhibited lower diiodomethane contact angles (53°, 54° and 62°, respectively), they corresponded to higher non-polar Lifshitz–van der Waals components and also higher surface energy values according to the vOCG approach. Higher diiodomethane contact angles for the control, chromic acid, water and smoothest surfaces corresponded to a lower non-polar Lifshitz–van der Waals component of surface energy for both surface energy models.

The use of the water receding contact angle in the surface energy determinations caused an increase in the acid–base component of the surface energy for almost all the treated surfaces when the vOCG approach and the Chang model were used; however, this increase was larger when the vOCG approach was used except for the chromic acid treatment. For the chromic acid treatment the increase in the acid–base component was considerably higher when the Chang model was used; according to this model, the repulsive or attractive interactions between acidic and basic components for chromic acid treatment have great influence on the total surface energy.

The chromic acid treatment of the WPC surfaces presented an increase in the oxygen content on the surfaces, had one of the highest values of surface energy (according to the Chang model) and displayed also one of the highest increases in shear strength. These findings suggest that the strong bond of the WPC with the epoxy resin should be attributed to acid–base interactions. Apparently, chromic acid oxidizes and/or removes (through etching) the polypropylene and lubricant during the treatment process, creating oxygen containing functional groups that improve adhesive bonding. According to the Chang model, the resulting surfaces were amphoteric; so, in addition to the anionic groups formed through oxidation (e.g., carboxylic groups), some cationic groups must also be formed (potentially salt formation).

For flame, water–flame and flame–water treatments, an increase in the degree of surface oxidation was found, and in general, the acid–base component of the surface energy showed an increase when the water receding contact angle was used in the surface energy determinations. Using the water advancing contact angle, the increase in surface energy was attributed to the increase in the non-polar Lifshitz–van der Waals component of the surface energy. The increase in shear strength for these treatments is closely related to the increase in surface oxygen concentration and the corresponding increase in surface energy. As shown by Gramlich *et al.* [15], after water application, swelling of wood pockets on the surface occurred, and this swelling remained after the drying process creating greater surface area for wood–epoxy interactions. For flame–water and water–flame treatments the increased surface area of wood particles on the surface likely improved the bondability

because of the high compatibility between wood and epoxy resin, in addition to flame oxidation of the polypropylene and lubricant surface.

For flame-treated samples and also for the chromic acid treatment, the increase in shear strength could be attributed to the increase in surface energy, but also because through the treatments some WPC surface irregularities might have been removed. As such, the high shear strength may also be due to a contribution from micro-mechanical interlocking. It is noted that to obtain good adhesive bonding an intimate contact must be reached such that van der Waals interaction and/or the acid–base interactions can effectively occur.

Heat treatment presented almost no increase in the acid–base component of the surface energy compared to untreated surfaces and only a slight increase in the non-polar Lifshitz–van der Waals component of surface energy for using both water advancing and receding contact angles. Shear strength properties of these samples showed no increase compared to control samples.

Water treatment presented a 72% increase in the acid–base component of the surface energy compared to untreated surfaces, when the water receding contact angle was used in the surface energy determinations. Shear strength properties in this case presented an increase of 31% compared to control samples.

For mechanical treatments (P60 and P220) an increase of more than 100% in the acid–base component of the surface energy was found when the water receding contact angle was used for surface energy determinations, and when the vOCG approach was used as a model. The shear strength for the P60- and P220-treated samples presented an increase of 30% and 100%, respectively, compared to control samples. It is postulated that lower roughness and greater uniformity of the abraded WPC surfaces improved the effective contact of these surfaces with the epoxy resin, and improved their bond shear strength. The increase in shear strength, therefore, may potentially be attributed to improvement in micro-mechanical interlocking, and also to a more intimate contact between the epoxy resin and the functional groups containing oxygen. Evidence for contact between the epoxy resin and wood is found in the increased number of samples with wood in the bondline for the smoother surfaces (as presented in Table 10). The large difference in shear strengths found for the P60 and P220 (smoothest) treatments indicates that the surface roughness plays an important role in the bondability of WPCs and is a subject of continued research.

Based on the surface energy results found for the specific components of the WPCs formulation (polypropylene, coupling agent, colorant and lubricant), the low surface energy of WPC surfaces is most likely attributed to the polypropylene and lubricant components. The lubricant used in the preparation of the WPCs studied was a blend of complex modified fatty acid esters; as such, the lubricant comprises long hydrocarbon chains and a functional group composed of carbon, hydrogen and oxygen. Lubricants are added to the WPC mixture to improve the flow in the extruder, as well as improve the finished properties of the WPC. According to the Chang model, polypropylene exhibited an amphoteric nature; this

characteristic, similar to that found for polyethylene [23], may be attributed to the additives incorporated in their commercial formulation, such as antistatic agents or antioxidants. The amphoteric nature of the coupling agent, which corresponds to a modified polypropylene, is attributed to its functional groups. In the case of the colorant, which consists of a mixture of polyethylene, pigments and UV inhibitor, the Chang model displayed a low acid–base contribution and a basic nature. For the lubricant, although the vOCG approach showed a high acid–base contribution (4.66 mJ/m^2) and the Chang model gave a low acid–base contribution (-0.46 mJ/m^2), the total surface energy was the lowest for both models (23.3 mJ/m^2 and 18.2 mJ/m^2, respectively).

As shown in Fig. 8, the surface energy values correlate strongly with the oxidized carbon concentration on the surfaces as well as the shear strength. Indeed, using the Chang model for the surface energy analysis it is noted that the highest surface energy corresponds to the highest shear strength and the highest percentages of oxidized carbon; however, the large increase in oxidized carbon (or high oxygen concentration) displayed by surfaces treated with chromic acid did not show increase in the same proportion for either the surface energy or the shear strength.

5. CONCLUSIONS

Nearly all the treatments applied to the WPC surfaces improved their bondability to the epoxy adhesive. Mechanical treatments as a complement to the treatments performed and presented in the earlier paper [15] increased the shear strength of WPCs and epoxy resins; the smoothest surfaces exhibit higher mechanical properties and the results indicate that the wood component of WPCs causes the increase in their bondability with epoxy resin. Increases in the acid–base component of the surface energy display a close relationship with increases in shear strength measurements. The thermodynamic and spectroscopic techniques employed to characterize the surfaces after the treatments indicated that oxidation of WPC surfaces increased the total surface energy and improved their bondability with the epoxy adhesive. The use of the water advancing contact angles in the surface energy determinations had a higher impact on the non-polar Lifshitz–van der Waals component of the surface energy (γ_s^{LW}); conversely, the water receding contact angles had a higher impact on the acid–base component of the surface energy (γ_s^{AB}). The total surface energy changed only slightly when the advancing or receding water contact angle was used in the vOCG approach or the Chang model. Contact angle analysis employing the vOCG approach and the Chang model revealed that WPCs exhibit a low surface energy of approximately 21 mJ/m^2, likely due to the polypropylene matrix and the lubricant added to the composite during their manufacture.

Acknowledgements

Funding for this work was provided by the United States Coast Guard, Contract No. DTCG32-03-C-R00013 (Advanced Engineered Lumber Pier and Retaining Wall for CG Shore Facilities II, Federal Highway Administration (FHWA)), Contract No. DTFH61-06-C-0064 (The Structural Use of WPCs in Transportation Applications) and the National Science Foundation under Grant No. EPS-05-54545.

REFERENCES

1. J. Winandy, N. Stark and C. M. Clemons, *Proc. of the 5th Global Wood and Natural Fibre Composites Syposium*, pp. A6-1–A6-9, Kassel (2004).
2. S. A. Page, J. C. Berg and J. A. Månson, *J. Adhesion Sci. Technol.* **15**, 153–170 (2001).
3. Q. Shen, J. Nylund and J. B. Rosenholm, *Holzforschung* **52**, 521–529 (1998).
4. G. M. Wu, C. H. Hung and S. J. Liu, *J. Polym. Res.* **11**, 31–36 (2004).
5. A. Rochette, M. Bousmine and A. Lavoie, *J. Composite. Mater.* **36**, 925–940 (2002).
6. A. Bhurke and L. T. Drzal, *Proc. ANTEC Annual Technical Conference of the Society of Plastics Engineers*, pp. 1173–1177, Nashville, TN (2003).
7. T. Ogawa, H. Mukai and S. Osawa, *J. Appl. Polym. Sci.* **79**, 1162–1168 (2001).
8. D. Gardner, S. O'Neill, M. Peterson and J. Robinson, *Proc. 8th International Conference on Wood Fiber–Plastic Composites*, pp. 173–178, Madison, WI (2005).
9. A. P. Pijpers and R. J. Meier, *J. Electron Spectrosc. Relat. Phenom.* **21**, 299–313 (2001).
10. E. Papirer, D. Y. Wu and J. Schultz, *J. Adhesion Sci. Technol.* **7**, 343–362 (1993).
11. M. Strobel, M. C. Branch, M. Ulsh, R. S. Kapaun, S. Kirk and C. Lyons, *J. Adhesion Sci. Technol.* **10**, 515–539 (1996).
12. M. M. Strobel, N. Sullivan, M. Branch, V. Jones, J. Park, M. Ulsh, J. M. Strobel and C. Lyons, *J. Adhesion Sci. Technol.* **15**, 1–21 (2001).
13. M. Zenkiewicz, *J. Adhesion Sci. Technol.* **15**, 63–70 (2001).
14. E. Sheng, I. Sutherland, D. M. Brewis and R. J. Heath, *Appl. Surface Sci.* **78**, 249–254 (1994).
15. W. Gramlich, D. Gardner and D. Neivandt, *J. Adhesion Sci. Technol.* **20**, 1873–1887 (2006).
16. B. S. Gupta, Development of a coating technology for wood plastic composites, Master of Science in Material Science and Engineering, Chapter 3, pp. 42–86. Washington State University, Pullman, WA (2006).
17. D. J. Neivandt, M. L. Gee, C. Tripp and M. L. Hair, *Langmuir* **13**, 2519–2526 (1997).
18. L. M. Matuana, J. J. Balatinecz, R. N. Sodhi and C. B. Park, *Wood Sci. Technol.* **35**, 191–201 (2001).
19. W. Tze, G. Bernhardt, D. J. Gardner and A. W. Christiansen, *Int. J. Adhesion Adhesives*. **26**, 550–554 (2006).
20. C. J. van Oss, M. K. Chaudhury and R. J. Good, *Adv. Colloid Interface Sci.* **28**, 35–64 (1987).
21. C. Della Volpe and S. Siboni, *J. Colloid Interface Sci.* **195**, 121–136 (1997).
22. W. V. Chang and F. Chen, *Polym. Mater. Sci. Eng.* **61**, 607–613 (1989).
23. W. V. Chang and X. Qin, in: *Acid-Base Interactions: Relevance to Adhesion Science and Technology*, K. L. Mittal (Ed.), Vol. 2, pp. 5–53. VSP, Utrecht (2000).
24. D. J. Gardner, *Wood Fiber Sci.* **28**, 422–428 (1996).
25. D. J. Gardner, S. Q. Shi and W. T. Tze, in: *Acid-Base Interactions: Relevance to Adhesion Science and Technology*, K. L. Mittal (Ed.), Vol. 2, pp. 363–383. VSP, Utrecht (2000).
26. M. Wålinder, *Holzforschung* **56**, 363–371 (2002).
27. G. Sinn, M. Gindl, A. Reiterer and S. Stanzl-Tschegg, *Holzforschung* **58**, 246–251 (2004).
28. M. Wålinder and D. J. Gardner, *J. Adhesion Sci. Technol.* **16**, 1625–1649 (2002).

29. M. E. Shanahan and C. Bourges, *Intl. J. Adhesion Adhesives* **14**, 201–205 (1994).
30. D. Baptista, Assessment of water penetration resistance of coatings on wood by droplet dynamic analysis. Master of Science (in Forestry), pp. 80–117. University of Maine, Orono, ME (2005).